Oct 17th, 12:00 AM

Comparison of the Distortional Buckling Method for Flexural Members with Tests

Colin A. Rogers

R. M. Schuster

Thirteenth International Specialty Conference on Cold-Formed Steel Structures
St. Louis, Missouri U.S.A., October 17-18, 1996

COMPARISON OF THE DISTORTIONAL BUCKLING METHOD FOR FLEXURAL MEMBERS WITH TESTS

G.J. Hancock[1], C.A. Rogers[2] and R.M. Schuster[3]

SUMMARY

For thin-walled flexural members composed of certain geometric proportions and/or made of high-strength steel, a mode of buckling at half-wavelengths intermediate between local buckling and flexural-torsional or flexural buckling can occur. The mode is most common for edge (lip) stiffened members such as C and Z-sections, and involves rotation of the lip-flange component about the flange-web junction. This mode is commonly called distortional buckling.

Presented in this paper is a design method for distortional buckling of flexural members recently submitted for ballot with the AISI Specification Committee for Cold-Formed Steel Structures. Currently, the North American Cold-Formed Steel Design Standards do not contain such a distortional buckling provision. The distortional buckling procedure is compared with the current North American Design Standards using the results of beam tests carried out at the University of Waterloo and data available in the literature. Statistical results of the investigation indicate that the distortional buckling method is slightly conservative yet provides a better fit to the test data in comparison with current Design Standards. More importantly, the distortional buckling procedure accounts for recently observed significantly unconservative test results. It is recommended that the design method for the distortional buckling of flexural members, using Strength Curve 1 as presented herein, be adopted by the North American Design Standards.

1 INTRODUCTION

Distortional buckling of compression members (under uniform stress) such as C-sections usually involves rotation of the lip-flange components about the flange-web junctions in opposite directions as shown in Fig. 1(a). The web and lip-flange component buckling deformations, along with a possible translation of the entire section in a direction normal to the web, occur at the same half-wavelength. Web buckling involves single curvature transverse bending of the web. Distortional buckling of compression members (under uniform stress) has been investigated in detail by Hancock[1] mainly for sections used in steel storage racks, Lau & Hancock[2,3,4] for a range of different C and rack sections, and by Kwon & Hancock[5,6] for high strength steel channel sections with intermediate stiffeners.

Distortional buckling of flexural members such as C and Z-sections usually involves rotation

[1]BHP Steel Professor of Steel Structures, School of Civil and Mining Engineering, University of Sydney, Australia.
[2]Ph.D. Research Student, School of Civil and Mining Engineering, University of Sydney, Australia.
Former M.A.Sc. Research Student, Department of Civil Engineering, University of Waterloo, Canada.
[3]Professor of Structural Engineering, Department of Civil Engineering, University of Waterloo, Canada.

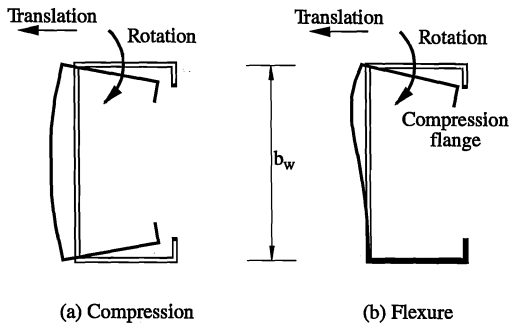

Figure 1. Distortional Buckling Modes

of only the compression lip-flange component about the flange-web junction, as shown in Fig. 1(b). The web and lip-flange component buckling deformations, along with a possible translation of the compression flange in a direction normal to the web, occur at the same half-wavelength. Web buckling involves double curvature transverse bending of the web. The purpose of this paper is to describe the rationale of the design method for distortional buckling of flexural members and to compare this method with available test data. It is also the intent to submit this proposed design method for inclusion in the Canadian Standards Association (CSA) S136 Standard[7] and the American Iron and Steel Institute (AISI) Specification[8] for Cold-Formed Steel Structures. The method presented herein is an improvement of the design method for distortional buckling of flexural members previously outlined by Hancock[9] for use in the Draft Australian / New Zealand Standard for Cold-Formed Steel Structures[10].

2 Elastic Distortional Buckling Stress Formulation

A paper by Lau & Hancock[11] provides distortional buckling formulae for channel columns based on a simple flange buckling model where the flange is treated as a thin-walled compression member undergoing flexural-torsional buckling, as shown in Fig. 2. The torsional restraint stiffness, k_ϕ, represents the torsional restraint of the web which is in pure compression, and the translational restraint stiffness, k_x, represents the resistance to translational movement of the section in the distortional buckling mode. As a result of the compressive stress in the web, the model includes a reduction in the torsional restraint stiffness, k_ϕ, provided by the web. The model is not limited to simple lip-flange combinations as shown in Fig. 2, but may involve complex lips with sloping stiffeners and/or return lips. In the Lau and Hancock model, it is assumed that the value of the translational spring stiffness, k_x, is zero so that the flange is free to translate in the x-direction in the buckling mode. The equation for the torsional restraint stiffness, k_ϕ, is given by Lau & Hancock as,

$$k_\phi = \frac{Et^3}{5.46\left(b_w + 0.06\lambda\right)}\left[1 - \frac{1.11 f_{od}'}{Et^2}\left(\frac{b_w^2\lambda}{b_w^2 + \lambda^2}\right)^2\right], \qquad (1)$$

where E is the modulus of elasticity and t is the thickness. In Eq. 1, λ is the half-wavelength of the distortional buckle which is given Eq. 2.

$$\lambda = 4.80\left(\frac{I_{xf} b_f^2 b_w}{t^3}\right)^{0.25} \qquad (2)$$

The symbol I_{xf} is defined in Appendix 'A', and the term f_{od}' is the compressive stress in the web at distortional buckling, computed assuming k_ϕ is zero. The computation process requires two steps due to the incorporation of f_{od}' in Eq. 1.

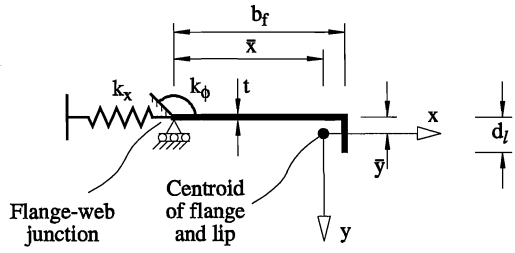

Figure 2. Flange Elastically Restrained Along Flange-Web Junction

The Lau & Hancock formulae for sections in compression[11] were modified so that they apply to the case of distortional buckling in flexure, as shown in Fig. 1(b). If the web of the C-section in compression in Fig. 1(a) is treated as a simply supported beam in flexure, as shown in Fig. 3(a), then the rotational stiffness at the end is *2EI/L*, as a result of the equal and opposite end moments. If the web of the C-section in flexure in Fig. 1(b) is treated as a beam simply supported at one end and built in at the other, as shown in Fig. 3(b), then the rotational stiffness at the end is *4EI/L*. Hence, it can be concluded that the change in end restraint from Fig. 1(a) to Fig. 1(b) will approximately double the torsional restraint stiffness, k_ϕ.

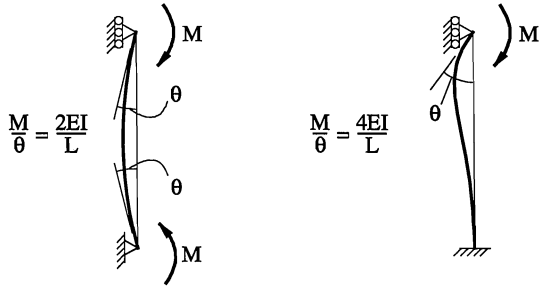

(a) Symmetric Bending

(b) Asymmetric Restrained Bending

Figure 3. Approximate Web Behaviour as a Beam in Flexure

Further, the width of the buckled section of the web is substantially reduced compared with the full web width, hence, the ratio of the buckle half-wavelength to buckle width is significantly increased since the distortional buckle half-wavelength remains relatively unchanged. For the original distortional buckling method of flexural members presented by Hancock[9], the compressive stress in the web was not assumed to have a significant effect on

reducing the torsional restraint stiffness, k_ϕ. However, for certain sections with web flat width ratios, *h/t*, above 150 and narrow flange elements it is possible for the buckle width of the web to extend past the centroid of the section, thus, reducing the torsional restraint on the lip-flange component. For this reason a further modification to Eq. 1 is made in this paper with the assumption that the web element is under a stress gradient caused by flexure in the member. The plate buckling coefficient, *k*, of a web element under pure in-plane bending varies as a function of the aspect ratio. Timoshenko & Gere listed numerical values of *k* for an element under pure bending for various aspect ratios (see Timoshenko & Gere Table 9-6 [12]). The resulting flange-web junction torsional restraint stiffness used in this paper (see Eq. 3 and Eq. A8 of Appendix 'A') was determined by modifying the denominator of Eq. 1, $(b_w^2 + \lambda^2)^2$, with the plate buckling coefficients described by Timoshenko & Gere to include a reduction factor based on the compressive stresses in the web.

$$k_\phi = \frac{2Et^3}{5.46\left(b_w + 0.06\lambda_d\right)}\left[1 - \frac{1.11 f_{ed}'}{Et^2}\left(\frac{b_w^4\lambda_d^2}{12.56\lambda_d^4 + 2.192b_w^4 + 13.39\lambda_d^2 b_w^2}\right)\right] \qquad (3)$$

The equation for the half-wavelength of the distortional buckle, Eq. 2, was revised by Hancock[9] to account for the web element which is under flexure rather than compression (see Eq. A2 of Appendix 'A'). Hancock's revision remains unchanged in this paper.

Two steps are required for this proposed distortional buckling procedure for flexural members. Initially the flange-web torsional restraint stiffness, k_ϕ, is calculated using Eq. 3, based on an initial assumption of the elastic distortional buckling stress, f_{ed}' (Eq. A7 of Appendix 'A'), which does not include the torsional restraint term in the α_1 equation (see Eq. A4 of Appendix 'A'). If the web torsionally restrains the lip-flange component, i.e., $k_\phi \geq 0$, the second step uses this value of the flange-web torsional restraint stiffness in the updated α_1 term (see Eq. A9 of Appendix 'A'). The final elastic distortional buckling stress, f_{ed} (Eq. A10 of Appendix 'A'), is determined using the updated α_1 and α_3 equations (see Eqs. A9 and A6 of Appendix 'A'). The second step differs only if the lip-flange component torsionally restrains the web, i.e., $k_\phi < 0$. In this case the k_ϕ term is recalculated without an initially assumed elastic distortional buckling stress (see Eq. A11 of Appendix 'A'). As for the previous case, the final elastic distortional buckling stress, f_{ed}, is determined using the updated α_1 and α_3 equations. The entire distortional buckling method for flexural members is fully described in Appendix 'A'.

Calculation of the elastic distortional buckling stress is dependent on the half-wavelength of the distortional buckle, λ_d. The calculated λ_d is used when the lip-flange component is able to rotate about the flange-web junction without restraint from any connective elements other than the web. When the lip-flange component is additionally restrained, the lesser value of the calculated λ_d and measured distance between restraints, λ_m, is used.

3 Strength Design Formulation

Strength design curves were derived from test data in Kwon & Hancock[6] and are summarised in Hancock et al.[13]. They allow for the interaction of buckling and yielding, as well as post-buckling strength in the distortional mode. The equations for the inelastic critical stress, f_c, are given for two strength design curves by Eqs. A12 to A15 of Appendix 'A'. The

inelastic critical stress is a function of the yield stress, f_y, and the elastic distortional buckling stress, f_{ed}. Equations A12 and A13 of Appendix 'A' are currently proposed as Strength Curve 1 for inclusion in the AISI Specification[8], with an alternate proposal (Strength Curve 2) given by Eqs. A14 and A15 of Appendix 'A'. The AISI proposed Strength Curve 1 for distortional buckling more accurately reflects the test data for flexural sections with an edge-stiffened flange. The alternate proposal, which is based on tests of compression members[11], gives approximately a 4% to 5% lower value for the predicted nominal buckling resistance of flexural members.

The distortional design method differentiates between local and distortional buckling behaviour when the section is such that the web torsionally restrains the lip-flange component, i.e., $k_\phi \geq 0$ (Eq. 3 or Eq. A8). In this instance, the nominal moment resistance, M_n, is calculated using the elastic section modulus of the full unreduced section for the extreme compression fibre, S_f, and the inelastic critical stress, f_c, (see Eq. A16 of Appendix 'A'). This moment strength calculation assumes that distortional buckling does not interact with local buckling, therefore the proposed S136 Standard[7] and proposed AISI Specification[8] distortional buckling methods yield the same result. However, it is assumed that local and distortional buckling interact when the lip-flange component torsionally restrains the web, i.e., $k_\phi < 0$ (Eq. 3 or Eq. A8). The nominal moment resistance is derived from the inelastic critical stress, f_c, and the elastic section modulus of the effective section, S_e, calculated at stress f_c in the extreme compression fibre (see Eq. A17 of Appendix 'A'). The effective section modulus is determined with the plate buckling coefficient for the flange set at $k = 4.0$ in the effective width equation for local buckling, and the assumed constant stress for the edge stiffener set at the maximum compression stress in the section, i.e., f_c. The results obtained from this local buckling calculation differ for the proposed S136 Standard and the proposed AISI Specification distortional buckling procedures. This difference arises because the method used to calculate the effective width of the web under a stress gradient has been modified in the S136 Standard. The AISI Specification results in a slightly larger effective section modulus in comparison to the S136 Standard due to a change in the distribution of the effective width of the web.

4 Applicable Waterloo and Available Test Data

Fifty-nine beam specimens were tested in the structures laboratory at the University of Waterloo. Of these specimens, forty-nine of the sections had edge-stiffened flanges and were applicable to this study, see Rogers[14]. Numerous investigations regarding the flexural behaviour of C and Z-sections were reviewed and summarised. The available test specimens were required to meet the following criteria; 1) the cross-section was either a C or a Z-shape, 2) adequate lateral support was provided during testing, 3) sections did not have web perforations, and 4) all edge stiffeners were simple lips at right angles to the flange. Data from the following researchers was included; Cohen[15], Desmond et al.[16], LaBoube & Yu[17], Moreyra & Peköz[18], Schardt & Schrade[19], Schuster[20], Shan et al.[21], Willis & Wallace[22], and Winter[23].

The distortional buckling method presented in this paper requires a measurement of the distance between torsional restraints of the lip-flange component. Typically this information was not recorded for the available data used in this comparison. In most cases it was assumed that the lip-flange component was not torsionally restrained unless specific information was

given. Studies by Willis & Wallace[22] and others have shown that the extent of torsional restraint offered by a steel deck to the lip-flange component is dependent on the position of the screw fasteners. Since information on the position of the screw fasteners was usually not given, the lip-flange component was not considered to be torsionally restrained for tests where steel decking was used. Further detailed information regarding the applicable Waterloo and available test data can be found in Rogers[14].

5 Comparison of Waterloo and Available Test Data

The applicable Waterloo and available test data was combined and analysed, with the overall test-to-predicted bending moment statistical results for the local and distortional buckling procedures presented in Table 1. Both North American design formats are presented so that the statistical results obtained from this investigation can be compared using procedures which follow the same design philosophy with only a different effective width procedure for the web. Test-to-predicted bending moment ratios for individual test specimens by Rogers[14], Moreyra & Peköz[18], Schuster[20], Willis & Wallace[22], as well as six of twenty-nine specimens tested by Shan et al.[21] are listed in Tables B1 and B2 of Appendix 'B'. Statistical results of the bending moment comparison for test data from each of the individual researchers are given in Tables B1 to B4 of Appendix 'B'. Analysis of the test specimens was carried out without the use of cold-work of forming.

Table 1 gives the statistical information of the nominal bending moment test-to-predicted comparison using all of the test data. The S136 and AISI columns refer to the results obtained from local buckling procedures specified in the S136 Standard[7] and AISI Specification[8], respectively. The distortional columns refer to the distortional buckling method outlined in Appendix 'A', where the S136 web and AISI web refer to the local buckling procedure used when the lip-flange component torsionally restrains the web, i.e., $k_\phi < 0$. The combined S136 and combined AISI columns list the results obtained when the controlling method, i.e., local or distortional buckling is used. Tables B1 and B2 of Appendix 'B', which provide information for individual test specimens, also give the sign of the flange-web junction torsional restraint stiffness, k_ϕ, as well as indicate which distortional half-wavelength, λ_d, was used in the calculation procedure, i.e., the calculated (c) or measured (m) half-wavelength.

Table 1. M_T/M_P Ratios Waterloo & Available Data

	S136 M_T/M_P	Distortional (S136 Web) M_T/M_P	Combined S136 M_T/M_P	AISI M_T/M_P	Distortional (AISI Web) M_T/M_P	Combined AISI M_T/M_P
Strength Curve 1						
Avg.	1.067	1.097	1.106	1.021	1.088	1.095
No.	203	203	203	203	203	203
S.D.	0.111	0.107	0.100	0.120	0.116	0.108
C.o.V.	0.104	0.098	0.091	0.118	0.107	0.099
Strength Curve 2						
Avg.	1.067	1.146	1.150	1.021	1.137	1.141
No.	203	203	203	203	203	203
S.D.	0.111	0.116	0.109	0.120	0.126	0.119
C.o.V.	0.104	0.102	0.095	0.118	0.111	0.105

The overall statistical information for the Waterloo and available data indicates that the combined use of local and distortional buckling results in a slightly conservative prediction of the nominal moment resistance in comparison with local buckling procedures. However, the combined approach more accurately fits the data with decreased standard deviations and coefficients of variation. Furthermore, the combined approach accounts for recently observed significantly unconservative test results using the current North American Design Standards (see Tables B1 and B2 of Appendix 'B'). In an extreme case presented in this paper, industry standard C-sections tested by Schuster[20] were found to have nominal bending moment test-to-predicted ratios as low as 0.83 and 0.76 calculated using the S136 Standard[7] and AISI Specification[8], respectively (see Table B1 or B2 of Appendix 'B'). Use of the distortional buckling procedures for these sections, as well as other flexural test specimens where the bending moment resistance is over-predicted, increases the accuracy of the calculated nominal bending moment resistance (see Tables B1 and B2 of Appendix 'B').

The distortional buckling procedure relies on the use of a strength curve to account for the interaction of buckling and yielding, as well as post-buckling strength in the distortional mode. The distortional and combined overall statistical results obtained using Strength Curve 2 (Eqs. A14 and A15 of Appendix 'A') are more conservative in comparison to those obtained using Strength Curve 1 (Eqs. A12 and A13 of Appendix 'A') (see Table 1). It is therefore recommended that the combined local and distortional approach, using Strength Curve 1, be included in the North American Design Standards[7,8].

6 Conclusions

A design method for computing the distortional buckling bending moment resistance of flexural members has been presented. Currently, the North American Cold-Formed Steel Design Standards do not contain such a distortional buckling provision. This distortional buckling procedure has been compared with the current North American Design Standards using the results of beam tests carried out at the University of Waterloo and data available in the literature. Statistical results of the investigation indicate that the distortional buckling method is slightly more conservative in mean values yet more accurate in data fit in comparison with current design standards. More importantly, the distortional buckling procedure accounts for recently observed significantly unconservative test results. It is therefore recommended that the design method for the distortional buckling of flexural members, using Strength Curve 1 as presented herein, be adopted by the North American Design Standards.

Acknowledgements

The authors wish to thank the Canadian Sheet Steel Building Institute and the National Research Council's Industrial Research Assistance Programme for their financial support. The comments of Dr. James M. Fisher of Computerized Structural Design, Inc. and Ben W. Schafer of Cornell University are also appreciated.

REFERENCES

1) Hancock, G.J., "Distortional Buckling of Steel Storage Rack Columns", Journal of Structural Engineering, ASCE, 1985, 111(12), pp. 2770-2783.
2) Lau, S.C.W., Hancock, G.J., "Distortional Buckling Tests of Cold-Formed Channel Sections", Ninth International Specialty Conference on Cold-Formed Steel Structures, St Louis, Missouri, 1988, pp. 45-73.
3) Lau, S.C.W., Hancock, G.J., "Strength Tests and Design Methods for Cold-Formed Channel Columns Undergoing Distortional Buckling", Research Report No R579, School of Civil and Mining Engineering, University of Sydney, 1988.
4) Lau, S.C.W., Hancock, G.J., "Inelastic Buckling of Channel Columns in the Distortional Mode", Thin-Walled Structures, 1990, 10, pp. 59-84.
5) Kwon, Y.B., Hancock, G.J., "Design of Channels Against Distortional Buckling", Eleventh International Specialty Conference on Cold-Formed Steel Structures, St Louis, Missouri, 1992, pp. 323-352.
6) Kwon, Y.B., Hancock, G.J., "Strength Tests of Cold-formed Channel Sections Undergoing Local and Distortional Buckling", Journal of Structural Engineering, ASCE, 1992, 117(2), pp. 1786-1803.
7) S136-94, "Cold Formed Steel Structural Members", Canadian Standards Association, Rexdale (Toronto), Ontario, Canada, 1994.
8) American Iron and Steel Institute, "Specification for the Design of Cold-Formed Steel Structural Members", August 19, 1986 Edition with December 11, 1989 Addendum, Washington D.C., USA, 1989.
9) Hancock, G.J., "Design for Distortional Buckling of Flexural Members", Proceedings of the Third International Conference on Steel and Aluminium Structures", Istanbul, Turkey, 1995, pp. 275-283.
10) Standards Australia / Standards New Zealand, "Cold-formed steel structures (Revision of AS 1538-1988)",Committee Document BD/82/94-12, Sydney, Australia.
11) Lau, S.C.W., Hancock, G.J., "Distortional Buckling Formulas for Channel Columns", Journal of Structural Engineering, ASCE, 1987, 113(5), pp. 1063-1078.
12) Timoshenko, S.P., Gere, J.M., "Theory of Elastic Stability" Second Edition, McGraw-Hill Book Company Inc., New York, 1961.
13) Hancock, G.J., Kwon, Y.B., Bernard, E.S., "Strength Design Curves for Thin-Walled Sections Undergoing Distortional Buckling", Journal of Constructional Steel Research, Vol. 31, Nos. 2-3, 1994, pp. 169-186.
14) Rogers, C.A., "Local and Distortional Buckling of Cold Formed Steel Channel and Zed Sections in Bending", M.A.Sc. Thesis presented to the Department of Civil Engineering, University of Waterloo, Waterloo Ontario, May, 1995.
15) Cohen, J.M., "Local Buckling Behaviour of Plate Elements", A thesis presented to the Faculty of the Graduate School of Cornell University in partial fulfilment for the Degree of Doctor of Philosophy, Department of Structural Engineering., Cornell University, Ithaca N.Y., August 1987.
16) Desmond, T.P., Peköz, T., Winter, G., "Edge Stiffeners for Thin-Walled Members", Journal of the Structural Division, ASCE, Vol. 107, No. ST2, February 1981, pp 329-353.
17) LaBoube, R.A., Yu, W.W., "Webs for Cold-Formed Steel Flexural Members - Structural Behaviour of Beam Webs Subjected to Bending Stress", Final Report, Civil Engineering Study 78-1, Structural Series, University of Missouri-Rolla, Rolla, Missouri, June 1978.
18) Moreyra, M.E., Peköz, T., "Behavior of Cold-Formed Steel Lipped Channels Under Bending and Design of Edge Stiffened Elements", Research Report 93-4, School of Civil and Environmental Engineering, Cornell University, Ithaca N.Y., June 1993.
19) Schardt, R., Schrade, W., "Kaltprofil - Pfetten", Institut Für Statik, Technische Hochschule Darmstadt, Bericht Nr. 1, Darmstadt, 1982.
20) Schuster, R.M., "Testing of Perforated C-Stud Sections in Bending", Report for the Canadian Sheet Steel Building Institute, University of Waterloo, Waterloo Ontario, March 1992.
21) Shan, M.Y., LaBoube, R.A., Yu, W.W., "Behaviour of Web Elements with Openings Subjected to Bending, Shear and the Combination of Bending and Shear", Final Report, Civil Engineering Study 94-2 Structural Series, University of Missouri-Rolla, Rolla, Missouri, May 1994.
22) Willis, C.T., Wallace, B.J., "Behaviour of Cold-Formed Steel Purlins Under Gravity Loading", Journal of the Structural Division, ASCE, Vol. 116, No. 8, August 1990, pp. 2061-2069.
23) Winter, G., "Strength of Thin Steel Compression Flanges", Transactions, ASCE, Vol. 112, 1947, pp. 527-6576.

APPENDIX 'A'

NOMINAL BENDING MOMENT RESISTANCE FOR DISTORTIONAL BUCKLING

Step 1

$$\beta_1 = \bar{x}^2 + \left(\frac{I_{xf} + I_{yf}}{A_f}\right) \qquad \text{(Eq. A1)}$$

$$\lambda_d = 4.80\left(\frac{I_{xf} b_f^2 b_w}{2t^3}\right)^{0.25} \qquad \text{If } \lambda_m < \lambda_d \text{ then } \lambda_d = \lambda_m \qquad \text{(Eq. A2)}$$

$$\eta = \left(\frac{\pi}{\lambda_d}\right)^2 \qquad \text{(Eq. A3)}$$

$$\alpha_1 = \frac{\eta}{\beta_1}\left(I_{xf} b_f^2 + 0.039 J_f \lambda_d^2\right) \qquad \text{(Eq. A4)}$$

$$\alpha_2 = \eta\left(I_{yf} + \frac{2}{\beta_1}\bar{y} b_f I_{xyf}\right) \qquad \text{(Eq. A5)}$$

$$\alpha_3 = \eta\left(\alpha_1 I_{yf} - \frac{\eta}{\beta_1} I_{xyf}^2 b_f^2\right) \qquad \text{(Eq. A6)}$$

$$f_{ed}' = \frac{E}{2A_f}\left\{(\alpha_1 + \alpha_2) \pm \sqrt{(\alpha_1 + \alpha_2)^2 - 4\alpha_3}\right\} \quad \text{(smaller positive value)} \qquad \text{(Eq. A7)}$$

$$k_\phi = \frac{2Et^3}{5.46(b_w + 0.06\lambda_d)}\left[1 - \frac{1.11 f_{ed}'}{Et^2}\left(\frac{b_w^4 \lambda_d^2}{12.56\lambda_d^4 + 2.192 b_w^4 + 13.39\lambda_d^2 b_w^2}\right)\right] \qquad \text{(Eq. A8)}$$

Step 2

If $k_\phi \geq 0$ then:

$$\alpha_1 = \frac{\eta}{\beta_1}\left(I_{xf} b_f^2 + 0.039 J_f \lambda_d^2\right) + \frac{k_\phi}{\beta_1 \eta E} \qquad \text{(Eq. A9)}$$

$$\alpha_3 = \eta\left(\alpha_1 I_{yf} - \frac{\eta}{\beta_1} I_{xyf}^2 b_f^2\right) \qquad \text{(Eq. A6)}$$

$$f_{ed} = \frac{E}{2A_f}\left\{(\alpha_1 + \alpha_2) \pm \sqrt{(\alpha_1 + \alpha_2)^2 - 4\alpha_3}\right\} \quad \text{(smaller positive value)} \qquad \text{(Eq. A10)}$$

If $k_\phi < 0$ then:

$$k_\phi = \frac{2Et^3}{5.46(b_w + 0.06\lambda_d)} \qquad \text{(Eq. A11)}$$

$$\alpha_1 = \frac{\eta}{\beta_1}\left(I_{xf} b_f^2 + 0.039 J_f \lambda_d^2\right) + \frac{k_\phi}{\beta_1 \eta E} \qquad \text{(Eq. A9)}$$

$$\alpha_3 = \eta\left(\alpha_1 I_{yf} - \frac{\eta}{\beta_1} I_{xyf}^2 b_f^2\right) \qquad \text{(Eq. A6)}$$

$$f_{ed} = \frac{E}{2A_f}\left\{(\alpha_1 + \alpha_2) \pm \sqrt{(\alpha_1 + \alpha_2)^2 - 4\alpha_3}\right\} \quad \text{(smaller positive value)} \qquad \text{(Eq. A10)}$$

Strength Curve 1

For $f_{ed} > 2.2 f_y$

$$f_c = f_y \qquad \text{(Eq. A12)}$$

For $f_{ed} \leq 2.2 f_y$

$$f_c = f_y \sqrt{\frac{f_{ed}}{f_y}} \left(1 - 0.22 \sqrt{\frac{f_{ed}}{f_y}}\right) \qquad \text{(Eq. A13)}$$

Strength Curve 2

For $f_{ed} > 3.18 f_y$

$$f_c = f_y \qquad \text{(Eq. A14)}$$

For $f_{ed} \leq 3.18 f_y$

$$f_c = f_y \left(\frac{f_{ed}}{f_y}\right)^{0.6} \left(1 - 0.25 \left(\frac{f_{ed}}{f_y}\right)^{0.6}\right) \qquad \text{(Eq. A15)}$$

Nominal Moment Resistance

If $k_\phi \geq 0$ then:

$$M_n = S_f f_c \qquad \text{(Eq. A16)}$$

If $k_\phi < 0$ then:

$$M_n = S_e f_c \qquad \text{(Eq. A17)}$$

A_f = Full cross-sectional area of compression lip-flange component.
b_f = Compression flange width (see Fig. 2).
b_w = Web depth (see Fig. 1).
E = Modulus of Elasticity.
f_y = Yield stress.
I_{xf}, I_{yf} = Moment of inertia of compression lip-flange component about x, y axes respectively, where the x, y axes are located at the centroid of lip-flange component with x-axis parallel with flange (see Fig. 2).
I_{xyf} = Product moment of area of compression lip-flange component about x and y axes.
J_f = St. Venant torsion constant of compression lip-flange component.
$\bar{x}, \bar{y}$ = Distances from flange-web junction to centroid of compression lip-flange component in x, y directions respectively (see Fig. 2).
λ_m = Distance between restraints which limit rotation of the lip-flange component about the flange-web junction.
S_f = Elastic section modulus of the full unreduced section for the extreme compression fibre.
S_e = Elastic section modulus of the effective section calculated at stress f_c in the extreme compression fibre, with $k = 4.0$ for the flange, and $f = f_c$ for the edge stiffener. Note: the effective width calculation procedure for the web subject to a stress gradient differs for the S136 Standard and AISI Specification.

APPENDIX 'B'

Table B1. M_T/M_P Ratios Strength Curve 1

Specimen	M_T kN·m	S136 M_P kN·m	S136 M_T/M	Distortional (S136 Web) M_P kN·m	Distortional (S136 Web) M_T/M	Combined S136	Combined S136 M_T/M	AISI M_P kN·m	AISI M_T/M	Distortional (AISI Web) M_P kN·m	Distortional (AISI Web) M_T/M	Combined AISI	Combined AISI M_T/M	k_ϕ	λ_d
Rogers[14]															
C1-DW30-1	7.17	6.03	1.19	6.03	1.19	S	1.19	6.03	1.19	6.03	1.19	A	1.19	+	c
C1-DW40-1	7.48	6.25	1.20	6.25	1.20	S=D	1.20	6.25	1.20	6.25	1.20	A=D	1.20	+	c
C1-DW60-1	7.83	6.44	1.22	6.44	1.22	S=D	1.22	6.44	1.22	6.44	1.22	A=D	1.22	+	c
C1-DW80-1	8.43	6.84	1.23	6.84	1.23	S=D	1.23	6.84	1.23	6.84	1.23	A=D	1.23	+	c
C1-DW30-2	24.3	26.6	0.91	25.5	0.95	D	0.95	29.4	0.83	28.5	0.85	D	0.85	-	c
C1-DW40-2	24.9	26.8	0.93	26.1	0.95	D	0.95	29.8	0.84	29.2	0.85	D	0.85	-	c
C1-DW60-2	25.6	28.4	0.90	28.0	0.91	D	0.91	31.5	0.81	31.2	0.82	D	0.82	-	c
C1-DW80-2	26.1	29.3	0.89	28.6	0.91	D	0.91	32.7	0.80	32.1	0.81	D	0.81	-	c
C1-DW30-3	34.7	37.5	0.93	36.1	0.96	D	0.96	39.6	0.88	38.2	0.91	D	0.91	-	c
C1-DW40-3	35.9	38.8	0.93	36.9	0.97	D	0.97	41.0	0.88	39.2	0.92	D	0.92	-	c
C1-DW60-3	41.4	40.8	1.01	36.7	1.13	D	1.13	43.3	0.96	39.2	1.05	D	1.05	-	c
C2-DW20-1	4.19	3.73	1.12	3.61	1.16	D	1.16	3.88	1.08	3.61	1.16	D	1.16	+	c
C2-DW35-1	4.43	4.71	0.94	4.54	0.97	D	0.97	4.79	0.92	4.54	0.97	D	0.97	+	c
C2-DW45-1	5.16	4.84	1.07	4.48	1.15	D	1.15	4.86	1.06	4.48	1.15	D	1.15	+	c
C2-DW55-1	5.09	4.87	1.04	4.64	1.10	D	1.10	4.91	1.04	4.64	1.10	D	1.10	+	c
C2-DW65-1	5.57	5.01	1.11	5.10	1.09	S	1.11	5.09	1.10	5.10	1.09	A	1.10	+	m
C2-DW25-2	9.21	7.75	1.19	7.57	1.22	D	1.22	7.75	1.19	7.57	1.22	D	1.22	+	c
C2-DW40-2	10.4	8.45	1.23	8.42	1.24	D	1.24	8.45	1.23	8.42	1.24	D	1.24	+	c
C2-DW50-2	10.4	8.51	1.22	8.51	1.22	D	1.22	8.51	1.22	8.51	1.22	D	1.22	+	c
C2-DW60-2	11.0	8.81	1.24	8.81	1.25	D	1.25	8.81	1.24	8.81	1.25	D	1.25	+	c
C2-DW70-2	10.8	8.89	1.22	8.89	1.22	S	1.22	8.89	1.22	8.89	1.22	A	1.22	+	c
C2-DW80-2	11.2	9.16	1.23	9.16	1.22	S	1.23	9.16	1.23	9.16	1.22	A	1.23	+	c
C2-DW20-3	11.3	10.8	1.04	9.67	1.17	D	1.17	11.4	0.99	10.4	1.08	D	1.08	-	c
C2-DW35-3	12.2	12.9	0.94	11.5	1.06	D	1.06	13.7	0.89	11.5	1.06	D	1.06	+	c
C2-DW45-3	12.2	13.1	0.93	11.9	1.02	D	1.02	13.9	0.88	11.9	1.02	D	1.02	+	c
C2-DW55-3	13.3	13.4	0.99	12.6	1.05	D	1.05	14.2	0.94	12.6	1.05	D	1.05	+	m
C2-DW65-3	13.9	13.1	1.06	13.3	1.05	S	1.06	13.8	1.00	13.3	1.05	D	1.05	+	m
C2-DW80-3	13.2	12.6	1.05	12.2	1.09	D	1.09	13.4	0.99	13.1	1.01	D	1.01	-	m
C2-DW25-4	31.9	33.9	0.94	29.4	1.09	D	1.09	36.6	0.87	32.9	0.97	D	0.97	-	c
C2-DW40-4	36.1	37.3	0.97	33.7	1.07	D	1.07	40.6	0.89	37.1	0.97	D	0.97	-	c
C2-DW50-4	36.7	37.5	0.98	33.8	1.09	D	1.09	40.8	0.90	37.3	0.99	D	0.99	-	c
C2-DW60-4	40.0	39.2	1.02	35.4	1.13	D	1.13	42.8	0.94	39.2	1.02	D	1.02	-	c
C2-DW70-4	38.4	40.8	0.94	36.3	1.06	D	1.06	44.5	0.86	36.3	1.06	D	1.06	+	m
C2-DW80-4	39.6	41.0	0.97	36.5	1.08	D	1.08	44.9	0.88	40.6	0.97	D	0.97	-	m
C2R-DW20-1	4.16	3.64	1.14	3.45	1.21	D	1.21	3.71	1.12	3.45	1.21	D	1.21	+	c
C2R-DW35-1	5.05	4.77	1.06	4.45	1.14	D	1.14	4.78	1.06	4.45	1.14	D	1.14	+	c
C2R-DW45-1	5.22	4.97	1.05	4.63	1.13	D	1.13	4.97	1.05	4.63	1.13	D	1.13	+	c
C2R-DW55-1	5.26	4.93	1.07	4.75	1.11	D	1.11	4.92	1.07	4.75	1.11	D	1.11	+	c
C2R-DW65-1	5.49	4.81	1.14	4.81	1.14	D	1.14	4.82	1.14	4.81	1.14	D	1.14	+	m
C3-DW20-1	5.14	4.67	1.10	4.59	1.12	D	1.12	4.69	1.10	4.59	1.12	D	1.12	+	c
C3-DW30-1	5.37	5.38	1.00	5.22	1.03	D	1.03	5.37	1.00	5.22	1.03	D	1.03	+	m
C3-DW35-1	5.43	5.60	0.97	6.04	0.90	S	0.97	5.61	0.97	6.04	0.90	A	0.97	+	m
C3-DW45-1	5.37	5.36	1.00	6.14	0.87	S	1.00	5.36	1.00	6.14	0.87	A	1.00	+	m
C3-DW20-2	12.4	11.5	1.08	11.4	1.09	D	1.09	11.8	1.05	11.4	1.09	D	1.09	+	m
C3-DW30-2	13.4	13.4	1.00	13.8	0.97	S	1.00	13.8	0.97	13.8	0.97	D	0.97	+	m
C3-DW35-2	13.0	13.1	0.99	14.5	0.90	S	0.99	13.5	0.96	15.1	0.86	A	0.96	-	m
C3-DW45-2	13.4	13.1	1.02	15.1	0.89	S	1.02	13.4	1.00	15.7	0.86	A	1.00	-	m
C3-DW50-2	13.1	12.7	1.03	16.1	0.82	S	1.03	13.0	1.00	16.6	0.79	A	1.00	-	m
C3-DW60-2	13.2	12.3	1.07	16.6	0.79	S	1.07	12.6	1.05	17.2	0.77	A	1.05	-	m
Avg.			1.051		1.072		1.092		1.019		1.043		1.063		
No.			49		49		49		49		49		49		
S.D.			0.105		0.120		0.094		0.130		0.138		0.117		
C.o.V.			0.102		0.114		0.088		0.131		0.135		0.112		

Note: S, A, D refer to control by S136, AISI and distortional buckling design methods, respectively.
± refers to the sign of k_ϕ and c, m refer to either a calculated or measured λ_d, respectively.

Table B1. Cont. M_T/M_P Ratios Strength Curve 1

Specimen	M_T kN·m	M_P kN·m	S136 M_T/M	Distortional (S136 Web) M_P kN·m	Distortional (S136 Web) M_T/M		Combined S136 M_T/M	AISI M_P kN·m	AISI M_T/M	Distortional (AISI Web) M_P kN·m	Distortional (AISI Web) M_T/M		Combined AISI M_T/M	k_ϕ	λ_d
Moreyra & Peköz[18]															
A-W	14.0	15.1	0.93	14.0	1.00	D	1.00	16.2	0.86	14.0	1.00	D	1.00	+	c
A-TB	14.4	16.5	0.87	15.2	0.95	D	0.95	18.0	0.80	15.2	0.95	D	0.95	+	c
B-W	13.2	15.1	0.87	13.8	0.96	D	0.96	16.3	0.81	13.8	0.96	D	0.96	+	c
B-TB	14.0	15.5	0.91	14.6	0.96	D	0.96	17.0	0.82	14.6	0.96	D	0.96	+	c
C-W	15.6	13.9	1.12	13.3	1.17	D	1.17	15.4	1.02	13.3	1.17	D	1.17	+	c
C-TB	15.0	14.9	1.00	14.4	1.04	D	1.04	16.6	0.90	14.4	1.04	D	1.04	+	c
Avg.			0.951		1.014		1.014		0.869		1.014		1.014		
No.			6		6		6		6		6		6		
S.D.			0.097		0.086		0.086		0.081		0.086		0.086		
C.o.V.			0.131		0.109		0.109		0.121		0.109		0.109		
Schuster[20]															
BS1	8.46	9.07	0.93	8.52	0.99	D	0.99	10.3	0.82	8.52	0.99	D	0.99	+	c
BS2	8.61	9.07	0.95	8.52	1.01	D	1.01	10.3	0.84	8.52	1.01	D	1.01	+	c
CS1	9.05	10.8	0.83	10.0	0.90	D	0.90	11.9	0.76	10.0	0.90	D	0.90	+	c
CS2	9.05	10.9	0.83	10.0	0.90	D	0.90	11.9	0.76	10.0	0.90	D	0.90	+	c
CS3	9.29	10.8	0.86	10.0	0.93	D	0.93	11.9	0.78	10.0	0.93	D	0.93	+	c
Avg.			0.881		0.947		0.947		0.792		0.947		0.947		
No.			5		5		5		5		5		5		
S.D.			0.055		0.052		0.052		0.038		0.052		0.052		
C.o.V.			0.089		0.077		0.077		0.067		0.077		0.077		
Shan et al.[21]															
8A,14,7&8(N)	15.3	17.4	0.88	15.9	0.96	D	0.96	19.2	0.80	15.9	0.96	D	0.96	+	c
8A,14,9&10(N)	15.7	17.4	0.90	15.9	0.99	D	0.99	19.2	0.82	15.9	0.99	D	0.99	+	c
8A,20,1&2(N)	4.07	4.56	0.89	4.23	0.96	D	0.96	4.75	0.86	4.23	0.96	D	0.96	+	c
8A,20,3&4(N)	4.12	4.64	0.89	4.28	0.96	D	0.96	4.84	0.85	4.28	0.96	D	0.96	+	c
12B,16,1&2(N)	22.5	28.9	0.78	25.0	0.90	D	0.90	30.5	0.74	27.0	0.84	D	0.84	-	c
12B,16,3&4(N)	23.4	28.5	0.82	24.7	0.95	D	0.95	30.1	0.78	26.7	0.88	D	0.88	-	c
Avg.			1.027		1.070		1.074		0.983		1.066		1.067		
No.			29		29		29		29		29		29		
S.D.			0.120		0.104		0.104		0.134		0.112		0.112		
C.o.V.			0.122		0.101		0.100		0.141		0.109		0.109		
Willis & Wallace[22]															
1C2	9.78	10.3	0.95	10.1	0.97	D	0.97	11.4	0.86	10.1	0.97	D	0.97	+	c
1C3	10.6	10.4	1.02	9.93	1.07	D	1.07	11.5	0.92	9.93	1.07	D	1.07	+	c
1C4	11.0	10.2	1.08	9.61	1.14	D	1.14	11.3	0.97	9.61	1.14	D	1.14	+	c
1C5	13.0	11.6	1.12	10.9	1.19	D	1.19	12.8	1.01	10.9	1.19	D	1.19	+	c
Avg.			1.043		1.093		1.093		0.940		1.093		1.093		
No.			4		4		4		4		4		4		
S.D.			0.074		0.096		0.096		0.065		0.096		0.096		
C.o.V.			0.123		0.152		0.152		0.119		0.152		0.152		

Note: S, A, D refer to control by S136, AISI and distortional buckling design methods, respectively.
± refers to the sign of k_ϕ and c, m refer to either a calculated or measured λ_d, respectively.

Table B2. M_T/M_P Ratios Strength Curve 2

Specimen	S136 M_T kN·m	S136 M_P kN·m	S136 M_T/M	Distortional (S136 Web) M_P kN·m	Distortional (S136 Web) M_T/M	Combined S136	Combined S136 M_T/M	AISI M_P kN·m	AISI M_T/M	Distortional (AISI Web) M_P kN·m	Distortional (AISI Web) M_T/M	Combined AISI	Combined AISI M_T/M	k_ϕ	λ_d
Rogers[14]															
C1-DW30-1	7.17	6.03	1.19	5.93	1.21	D	1.21	6.03	1.19	5.93	1.21	D	1.21	+	c
C1-DW40-1	7.48	6.25	1.20	6.23	1.20	S=D	1.20	6.25	1.20	6.23	1.20	A=D	1.20	+	c
C1-DW60-1	7.83	6.44	1.22	6.44	1.22	S=D	1.22	6.44	1.22	6.44	1.22	A=D	1.22	+	c
C1-DW80-1	8.43	6.84	1.23	6.84	1.23	S=D	1.23	6.84	1.23	6.84	1.23	A=D	1.23	+	c
C1-DW30-2	24.3	26.6	0.91	24.9	0.98	D	0.98	29.4	0.83	27.9	0.87	D	0.87	-	c
C1-DW40-2	24.9	26.8	0.93	25.4	0.98	D	0.98	29.8	0.84	28.6	0.87	D	0.87	-	c
C1-DW60-2	25.6	28.4	0.90	27.2	0.94	D	0.94	31.5	0.81	30.5	0.84	D	0.84	-	c
C1-DW80-2	26.1	29.3	0.89	27.8	0.94	D	0.94	32.7	0.80	31.3	0.83	D	0.83	-	c
C1-DW30-3	34.7	37.5	0.93	35.2	0.99	D	0.99	39.6	0.88	37.4	0.93	D	0.93	-	c
C1-DW40-3	35.9	38.8	0.93	36.0	1.00	D	1.00	41.0	0.88	38.4	0.94	D	0.94	-	c
C1-DW60-3	41.4	40.8	1.01	35.8	1.16	D	1.16	43.3	0.96	38.4	1.08	D	1.08	-	c
C2-DW20-1	4.19	3.73	1.12	3.44	1.22	D	1.22	3.88	1.08	3.44	1.22	D	1.22	+	c
C2-DW35-1	4.43	4.71	0.94	4.40	1.01	D	1.01	4.79	0.92	4.40	1.01	D	1.01	+	c
C2-DW45-1	5.16	4.84	1.07	4.35	1.19	D	1.19	4.86	1.06	4.35	1.19	D	1.19	+	c
C2-DW55-1	5.09	4.87	1.04	4.51	1.13	D	1.13	4.91	1.04	4.51	1.13	D	1.13	+	c
C2-DW65-1	5.57	5.01	1.11	4.95	1.13	D	1.13	5.09	1.10	4.95	1.13	D	1.13	+	m
C2-DW25-2	9.21	7.75	1.19	7.34	1.25	D	1.25	7.75	1.19	7.34	1.25	D	1.25	+	c
C2-DW40-2	10.4	8.45	1.23	8.10	1.28	D	1.28	8.45	1.23	8.10	1.28	D	1.28	+	c
C2-DW50-2	10.4	8.51	1.22	8.28	1.26	D	1.26	8.51	1.22	8.28	1.26	D	1.26	+	c
C2-DW60-2	11.0	8.81	1.24	8.61	1.28	D	1.28	8.81	1.24	8.61	1.28	D	1.28	+	c
C2-DW70-2	10.8	8.89	1.22	8.67	1.25	D	1.25	8.89	1.22	8.67	1.25	D	1.25	+	c
C2-DW80-2	11.2	9.16	1.23	8.83	1.27	D	1.27	9.16	1.23	8.83	1.27	D	1.27	+	c
C2-DW20-3	11.3	10.8	1.04	9.34	1.21	D	1.21	11.4	0.99	10.1	1.12	D	1.12	-	c
C2-DW35-3	12.2	12.9	0.94	10.89	1.12	D	1.12	13.7	0.89	10.9	1.12	D	1.12	+	c
C2-DW45-3	12.2	13.1	0.93	11.35	1.08	D	1.08	13.9	0.88	11.3	1.08	D	1.08	+	c
C2-DW55-3	13.3	13.4	0.99	12.08	1.10	D	1.10	14.2	0.94	12.1	1.10	D	1.10	+	m
C2-DW65-3	13.9	13.1	1.06	12.75	1.09	D	1.09	13.8	1.00	12.7	1.09	D	1.09	+	m
C2-DW80-3	13.2	12.6	1.05	11.86	1.11	D	1.11	13.4	0.99	12.8	1.03	D	1.03	-	m
C2-DW25-4	31.9	33.9	0.94	28.47	1.12	D	1.12	36.6	0.87	32.0	1.00	D	1.00	-	c
C2-DW40-4	36.1	37.3	0.97	32.85	1.10	D	1.10	40.6	0.89	36.4	0.99	D	0.99	-	c
C2-DW50-4	36.7	37.5	0.98	32.92	1.11	D	1.11	40.8	0.90	36.5	1.01	D	1.01	-	c
C2-DW60-4	40.0	39.2	1.02	34.56	1.16	D	1.16	42.8	0.94	38.4	1.04	D	1.04	-	c
C2-DW70-4	38.4	40.8	0.94	34.64	1.11	D	1.11	44.5	0.86	34.6	1.11	D	1.11	+	m
C2-DW80-4	39.6	41.0	0.97	35.58	1.11	D	1.11	44.9	0.88	39.8	1.00	D	1.00	-	m
C2R-DW20-1	4.16	3.64	1.14	3.31	1.26	D	1.26	3.71	1.12	3.31	1.26	D	1.26	+	c
C2R-DW35-1	5.05	4.77	1.06	4.31	1.17	D	1.17	4.78	1.06	4.31	1.17	D	1.17	+	c
C2R-DW45-1	5.22	4.97	1.05	4.49	1.16	D	1.16	4.97	1.05	4.49	1.16	D	1.16	+	c
C2R-DW55-1	5.26	4.93	1.07	4.61	1.14	D	1.14	4.92	1.07	4.61	1.14	D	1.14	+	c
C2R-DW65-1	5.49	4.81	1.14	4.66	1.18	D	1.18	4.82	1.14	4.66	1.18	D	1.18	+	m
C3-DW20-1	5.14	4.67	1.10	4.40	1.17	D	1.17	4.69	1.10	4.40	1.17	D	1.17	+	c
C3-DW30-1	5.37	5.38	1.00	5.04	1.07	D	1.07	5.37	1.00	5.04	1.07	D	1.07	+	m
C3-DW35-1	5.43	5.60	0.97	5.87	0.93	S	0.97	5.61	0.97	5.87	0.93	A	0.97	+	m
C3-DW45-1	5.37	5.36	1.00	5.95	0.90	S	1.00	5.36	1.00	5.95	0.90	A	1.00	+	m
C3-DW20-2	12.4	11.5	1.08	10.41	1.19	D	1.19	11.8	1.05	10.4	1.19	D	1.19	+	m
C3-DW30-2	13.4	13.4	1.00	12.93	1.04	D	1.04	13.8	0.97	12.9	1.04	D	1.04	+	m
C3-DW35-2	13.0	13.1	0.99	14.11	0.92	S	0.99	13.5	0.96	14.8	0.88	A	0.96	-	m
C3-DW45-2	13.4	13.1	1.02	14.70	0.91	S	1.02	13.4	1.00	15.3	0.88	A	1.00	-	m
C3-DW50-2	13.1	12.7	1.03	15.62	0.84	S	1.03	13.0	1.00	16.2	0.81	A	1.00	-	m
C3-DW60-2	13.2	12.3	1.07	16.25	0.81	S	1.07	12.6	1.05	16.8	0.78	A	1.05	-	m
Avg.			1.051		1.106		1.122		1.019		1.075		1.092		
No.			49		49		49		49		49		49		
S.D.			0.105		0.122		0.098		0.130		0.143		0.123		
C.o.V.			0.102		0.113		0.089		0.131		0.136		0.115		

Note: S, A, D refer to control by S136, AISI and distortional buckling design methods, respectively.
± refers to the sign of k_ϕ and c, m refer to either a calculated or measured λ_d, respectively.

Table B2. Cont. M_T/M_P Ratios Strength Curve 2

Specimen	M_T kN·m	S136 M_P kN·m	S136 M_T/M	Distortional (S136 Web) M_P kN·m	Distortional (S136 Web) M_T/M	Combined S136	Combined S136 M_T/M	AISI M_P kN·m	AISI M_T/M	Distortional (AISI Web) M_P kN·m	Distortional (AISI Web) M_T/M	Combined AISI	Combined AISI M_T/M	k_ϕ	λ_d
Moreyra & Peköz[18]															
A-W	14.0	15.1	0.93	13.6	1.03	D	1.03	16.2	0.86	13.6	1.03	D	1.03	+	c
A-TB	14.4	16.5	0.87	14.6	0.99	D	0.99	18.0	0.80	14.6	0.99	D	0.99	+	c
B-W	13.2	15.1	0.87	13.3	0.99	D	0.99	16.3	0.81	13.3	0.99	D	0.99	+	c
B-TB	14.0	15.5	0.91	14.0	1.00	D	1.00	17.0	0.82	14.0	1.00	D	1.00	+	c
C-W	15.6	13.9	1.12	12.8	1.22	D	1.22	15.4	1.02	12.8	1.22	D	1.22	+	c
C-TB	15.0	14.9	1.00	13.8	1.09	D	1.09	16.6	0.90	13.8	1.09	D	1.09	+	c
Avg.			0.951		1.052		1.052		0.869		1.052		1.052		
No.			6		6		6		6		6		6		
S.D.			0.097		0.090		0.090		0.081		0.090		0.090		
C.o.V.			0.131		0.111		0.111		0.121		0.111		0.111		
Schuster[20]															
BS1	8.46	9.07	0.93	8.21	1.03	D	1.03	10.3	0.82	8.21	1.03	D	1.03	+	c
BS2	8.61	9.07	0.95	8.21	1.05	D	1.05	10.3	0.84	8.21	1.05	D	1.05	+	c
CS1	9.05	10.8	0.83	9.61	0.94	D	0.94	11.9	0.76	9.61	0.94	D	0.94	+	c
CS2	9.05	10.9	0.83	9.64	0.94	D	0.94	11.9	0.76	9.64	0.94	D	0.94	+	c
CS3	9.29	10.8	0.86	9.62	0.97	D	0.97	11.9	0.78	9.62	0.97	D	0.97	+	c
Avg.			0.881		0.985		0.985		0.792		0.985		0.985		
No.			5		5		5		5		5		5		
S.D.			0.055		0.051		0.051		0.038		0.051		0.051		
C.o.V.			0.089		0.073		0.073		0.067		0.073		0.073		
Shan et al.[21]															
8A,14,7&8(N)	15.3	17.4	0.88	15.4	1.00	D	1.00	19.2	0.80	15.4	1.00	D	1.00	+	c
8A,14,9&10(N)	15.7	17.4	0.90	15.4	1.02	D	1.02	19.2	0.82	15.4	1.02	D	1.02	+	c
8A,20,1&2(N)	4.07	4.56	0.89	3.97	1.03	D	1.03	4.75	0.86	3.97	1.03	D	1.03	+	c
8A,20,3&4(N)	4.12	4.64	0.89	4.02	1.02	D	1.02	4.84	0.85	4.02	1.02	D	1.02	+	c
12B,16,1&2(N)	22.5	28.9	0.78	24.2	0.93	D	0.93	30.5	0.74	26.2	0.86	D	0.86	-	c
12B,16,3&4(N)	23.4	28.5	0.82	23.9	0.98	D	0.98	30.1	0.78	25.9	0.90	D	0.90	-	c
Avg.			1.027		1.115		1.115		0.983		1.110		1.110		
No.			29		29		29		29		29		29		
S.D.			0.120		0.104		0.104		0.134		0.113		0.113		
C.o.V.			0.122		0.097		0.097		0.141		0.106		0.106		
Willis & Wallace[22]															
1C2	9.78	10.3	0.95	9.74	1.00	D	1.00	11.4	0.86	9.74	1.00	D	1.00	+	c
1C3	10.6	10.4	1.02	9.58	1.11	D	1.11	11.5	0.92	9.58	1.11	D	1.11	+	c
1C4	11.0	10.2	1.08	9.27	1.19	D	1.19	11.3	0.97	9.27	1.19	D	1.19	+	c
1C5	13.0	11.6	1.12	10.5	1.24	D	1.24	12.8	1.01	10.5	1.24	D	1.24	+	c
Avg.			1.043		1.135		1.135		0.940		1.135		1.135		
No.			4		4		4		4		4		4		
S.D.			0.074		0.103		0.103		0.065		0.103		0.103		
C.o.V.			0.123		0.157		0.157		0.119		0.157		0.157		

Note: S, A, D refer to control by S136, AISI and distortional buckling design methods, respectively.
± refers to the sign of k_ϕ and c, m refer to either a calculated or measured λ_d, respectively.

Table B3. Statistical Results M_T/M_P Ratios Strength Curve 1

Specimen	S136 M_T/M_P	Distortional (S136 Web) M_T/M_P	Combined S136 M_T/M_P	AISI M_T/M_P	Distortional (AISI Web) M_T/M_P	Combined AISI M_T/M_P
Cohen[15]						
Avg.	1.199	1.201	1.216	1.153	1.201	1.201
No.	14	14	14	14	14	14
S.D.	0.073	0.067	0.069	0.064	0.067	0.067
C.o.V.	0.066	0.061	0.062	0.060	0.061	0.061
Desmond et al.[16]						
Avg.	1.146	1.142	1.164	1.143	1.142	1.164
No.	4	4	4	4	4	4
S.D.	0.081	0.122	0.095	0.077	0.122	0.095
C.o.V.	0.123	0.185	0.141	0.117	0.185	0.141
LaBoube & Yu[17]						
Avg.	1.078	1.114	1.119	1.027	1.112	1.112
No.	52	52	52	52	52	52
S.D.	0.079	0.082	0.075	0.078	0.083	0.082
C.o.V.	0.075	0.075	0.069	0.077	0.076	0.075
Schardt & Schrade[19]						
Avg.	1.086	1.126	1.126	1.029	1.126	1.126
No.	25	25	25	25	25	25
S.D.	0.127	0.123	0.123	0.112	0.123	0.123
C.o.V.	0.122	0.114	0.114	0.113	0.114	0.114
Winter[23]						
Avg.	1.096	1.094	1.104	1.070	1.094	1.100
No.	15	15	15	15	15	15
S.D.	0.064	0.058	0.061	0.061	0.058	0.057
C.o.V.	0.063	0.057	0.059	0.062	0.057	0.055

Table B4. Statistical Results M_T/M_P Ratios Strength Curve 2

Specimen	S136 M_T/M_P	Distortional (S136 Web) M_T/M_P	Combined S136 M_T/M_P	AISI M_T/M_P	Distortional (AISI Web) M_T/M_P	Combined AISI M_T/M_P
Cohen[15]						
Avg.	1.199	1.260	1.261	1.153	1.260	1.260
No.	14	14	14	14	14	14
S.D.	0.073	0.069	0.069	0.064	0.069	0.069
C.o.V.	0.066	0.060	0.060	0.060	0.060	0.060
Desmond et al.[16]						
Avg.	1.146	1.194	1.208	1.143	1.194	1.208
No.	4	4	4	4	4	4
S.D.	0.081	0.142	0.124	0.077	0.142	0.124
C.o.V.	0.123	0.207	0.177	0.117	0.207	0.177
LaBoube & Yu[17]						
Avg.	1.078	1.167	1.168	1.027	1.165	1.165
No.	52	52	52	52	52	52
S.D.	0.079	0.086	0.085	0.078	0.089	0.089
C.o.V.	0.075	0.075	0.074	0.077	0.078	0.078
Schardt & Schrade[19]						
Avg.	1.086	1.208	1.208	1.029	1.208	1.208
No.	25	25	25	25	25	25
S.D.	0.127	0.134	0.134	0.112	0.134	0.134
C.o.V.	0.122	0.116	0.116	0.113	0.116	0.116
Winter[23]						
Avg.	1.096	1.134	1.135	1.070	1.134	1.135
No.	15	15	15	15	15	15
S.D.	0.064	0.066	0.066	0.061	0.066	0.066
C.o.V.	0.063	0.063	0.062	0.062	0.063	0.062